



# Effects of lignin content on the properties of lignocellulose-based biocomposites

F. Le Digabel<sup>a</sup>, L. Avérous<sup>b,\*</sup>

<sup>a</sup> UMR FARE INRA/URCA – BP 1039, 51687 Reims Cedex 2, France

<sup>b</sup> LIPHT-ECPM, University Louis Pasteur, 25 rue Becquerel, 67087 Strasbourg Cedex 2, France

Received 4 April 2006; accepted 22 April 2006

## Abstract

The paper is focused on the analysis of the behaviour of biocomposites (biodegradable composites) which are reinforced with different fillers fractions, with varying lignin contents. These materials have been carried-out by extrusion and injection moulding. The matrix, an aromatic copolyester (polybutylene adipate-co-terephthalate), is biodegradable. The lignocellulose fillers are a by-product of an industrial fractionation process of wheat straw. From the raw agro-material and by lignin extractions, various fillers fractions have been obtained by varying the fractionation conditions, both on the liquid media (aqueous or organic) and on the temperature. The fillers lignin contents vary from 30 to 14 wt% with a resultant increase of the cellulose content. We have analysed the impact of the different extraction conditions on the fillers surface and size distribution, and also on the final thermal and mechanical properties of the biocomposites. These materials present significant differences of behaviour which can fulfil some requirements for applications, such as non-food packaging or other short-lived applications (agriculture, sport...) where long-lasting polymers are not entirely adequate.

© 2006 Elsevier Ltd. All rights reserved.

**Keywords:** Biocomposite; Biodegradable; Lignocellulose fillers; Lignin extraction; Wheat straw

## 1. Introduction

Biocomposites (biodegradable composites) are obtained by blending together a biodegradable polymer and biodegradable fillers (e.g., lignocellulose fillers). Since both components are biodegradable, the composite as the integral part is also expected to be biodegradable (Mohanty, Misra, & Hinrichsen, 2000). Tailoring new composites within a perspective of eco-design or sustainable development is a philosophy that is applied to more and more materials. Ecological concerns have resulted in a resumed interest in renewable resources-based and/or composable products. It is the reason why material components such as natural fibers, biodegradable polymers can be considered as “interesting” – environmentally safe – alternatives.

The classification of these polymers has been shown elsewhere (Avérous, 2004). A large number of the biodegradable polymers are commercially available such as the biopolyesters (biodegradable polyesters). They show a large range of properties and at present, they can compete with non-biodegradable polymers in different industrial fields (e.g., packaging, agriculture, hygiene, and cutlery).

Lignocellulose-based fibers are widely used as biodegradable fillers. With their environmentally friendly character and some techno-economical advantages, these fibers motivate more and more different industrial sectors (e.g., automotive) to replace e.g., common glass fibers. Intrinsically, these natural fibers have a number of interesting mechanical and physical properties (Bledzki & Gassan, 1999; Mohanty et al., 2000; Rouilly & Rigal, 2002; Saheb & Jog, 1999). Table 1 shows that, according to the botanical source, these renewable materials present large variations in their composition. Main elements are cellulose, hemicellulose, and lignin which are known to present a very

\* Corresponding author. Tel.: +33 0 3 90 24 27 07; fax: +33 0 3 90 24 27 16.

E-mail address: [AverousL@ecpm.u-strasbg.fr](mailto:AverousL@ecpm.u-strasbg.fr) (L. Avérous).

Table 1  
Chemical composition (wt%) of vegetable fibers

	Cellulose	Lignin	Hemicellulose
<i>Bast fibers</i>			
Flax <sup>a</sup>	71	2	19
Hemp <sup>a</sup>	75	4	18
Jute <sup>a</sup>	72	13	13
<i>Leaf fibers</i>			
Abaca <sup>a</sup>	70	6	22
Sisal <sup>a</sup>	73	11	13
<i>Seed-hair fibers</i>			
Cotton <sup>a</sup>	93	—	3
Wheat straw <sup>a</sup>	51	16	26
<i>Lignocellulose fillers</i>			
LF	58	31	8

<sup>a</sup> Sources: Le Digabel, 2004; Young, 2004.

complex structure. Fig. 1 shows a tentative of schematic representation of wheat straw lignin proposed by Sun et al. (1997).

For short-term applications, biocomposites present strong advantages. Thus, a large number of papers has been published on this topic. Except some publications based on polysaccharide matrix e.g., plasticized starch (Avérous & Boquillon, 2004; Avérous, Fringant, & Moro, 2001), most of the studies (Avérous, 2004) are based on biopolyester matrices (Mohanty et al., 2000; Netravali & Chabba, 2003). For instance, aliphatic copolyesters have been used with cellulose fibers (Wollendorfer & Bader, 1998), bamboo fibers (Kitagawa, Watanabe, Mizoguchi,

& Hamada, 2002) or flax, oil palm, jute or ramie fibers (Wollendorfer & Bader, 1998). Aromatic copolyesters-based biocomposites have been less investigated. In a recent publication, lignocellulose fillers from wheat straw have been associated with different matrices such as aromatic copolyesters (Le Digabel, Boquillon, Dole, Monties, & Avérous, 2004).

This work is focused on the analysis of biocomposites based on treated lignocellulose fillers (TLF) displaying various lignin contents. The lignocellulose fillers (LF) are a by-product of an industrial wheat straw fractionation based on the extraction and the recovery of most of the hemicellulose sugars. Table 1 shows that, compared to wheat straw, LF present higher lignin content (30%) and a lower cellulose/lignin ratio, 1.9 compared to 3.2 for wheat straw. These low cost fillers (LF) are treated to reduce the lignin content and then to increase the cellulose concentration with the aim to analyze the impact of the lignin content variation on the biocomposites properties. By varying the extraction conditions, several fillers fractions displaying different lignin contents are obtained. To elaborate the biocomposites, these treated lignocellulose fillers (TLF) are mixed with polybutylene adipate-co-terephthalate (PBAT), a biodegradable aromatic copolyester. The aim of this paper is particularly focused on the analysis of the properties of both the treated fillers and the corresponding biocomposites. We have investigated the influence of the lignin extraction method, the impact of the lignin content on the fillers-matrix compatibility and on the final properties of these materials.

## 2. Experimental

### 2.1. Materials

The matrix, a biodegradable and aromatic copolyester (polybutylene adipate-co-terephthalate, PBAT) has been kindly supplied by Eastman (EASTAR BIO Ultra Copolyester 14766). Copolyester chemical structure is drawn in Fig. 2. The ratio between each monomer has been determined by <sup>1</sup>H NMR. We have measured 43% of butylene terephthalate and 57% of butylene adipate. Molecular weight ( $M_w$ ) and polydispersity index (IP) are 48,000 and 2.4, respectively. They have been determined by size exclusion chromatography (SEC). Melt flow index (MFI) is 13 g/10 mn at 190 °C/2.16 kg. PBAT density is 1.27 g/cm<sup>3</sup> at 23 °C.

The fillers are a by-product of an industrial fractionation process of wheat straw (ARD, Pomacle – France). These products are obtained from a multi-step process (Fig. 3). Two hundred and fifty kilograms of chopped wheat straw (10–15 cm) are introduced into a 1 m<sup>3</sup> reactor under high shearing to promote fibers fragmentation. Wheat straw is hydrolysed in acid medium (H<sub>2</sub>SO<sub>4</sub>, 0.1 N) under pressure (3.5 bars) at 130 °C, for 90 min (Roller, 1990). The soluble fraction (mostly hemicellulose sugars) is filtered and refined for further applications.

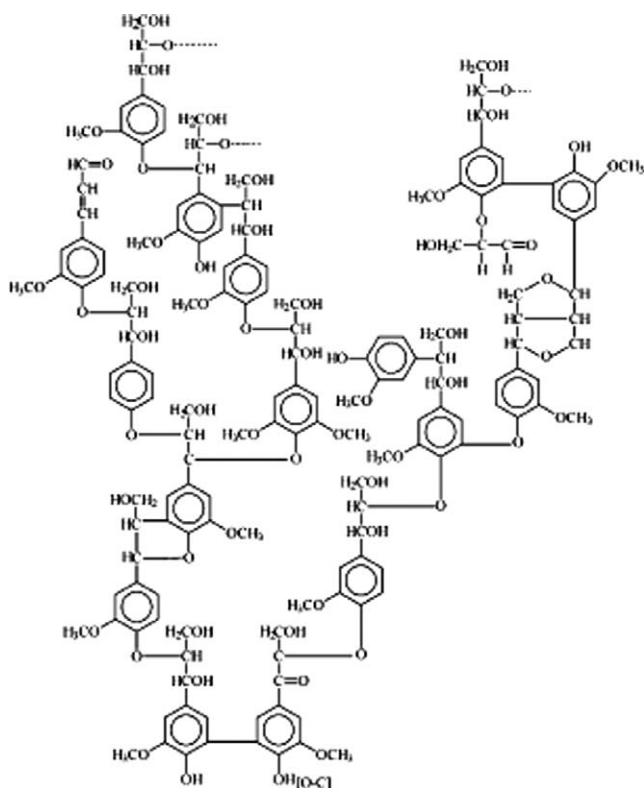


Fig. 1. Schematic representation of wheat straw lignin.

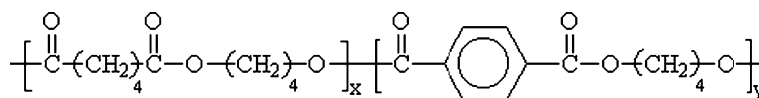


Fig. 2. Chemical structure of the copolyester (PBAT).

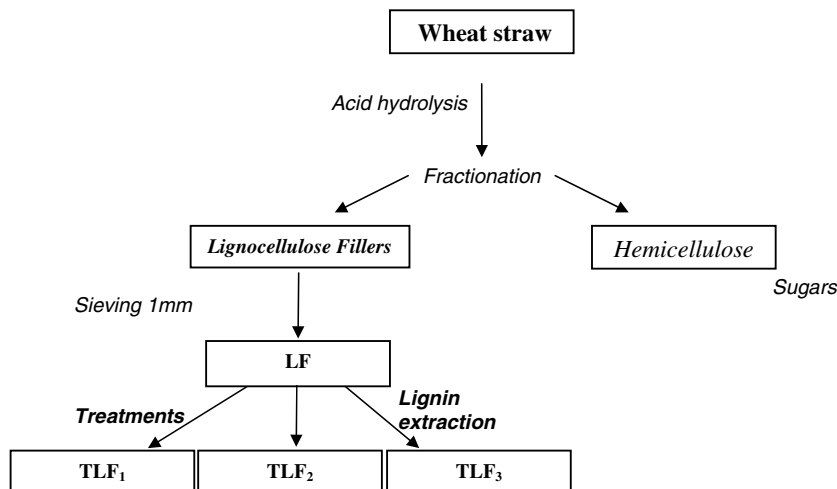


Fig. 3. Fillers fractions elaboration; wheat straw fractionation schema.

The insoluble fraction, the by-product called lignocellulose fillers, is neutralised and then washed and dried with a turbo-dryer (Alpha Vomm – Italy). The process yield, from the wheat straw to the lignocellulose fillers, is 33%. The dried fillers are sieved with a 1-mm grid to eliminate the biggest fillers (20 wt%). This product is named LF. Table 1 shows LF chemical composition. By HPLC analysis, the hemicellulose composition can be determined. Hemicellulose is composed with 96% of xylose, 3% of arabinose and 1% of mannose. LF density has been determined in a previous work (Le Digabel, 2004), at 1.45 g/cm<sup>3</sup>.

Two materials with opposite polar characters, cellulose (CF) and polypropylene (PP) have been used as materials references (hydrophilic and hydrophobic characters) for the determination of the surface tensions. Cellulose fibers (CF) from leafwood are supplied by Omya Rettenmier (JRS-Arbocel, Germany). Cellulose content is greater than 99.5 %. Residue on ignition at 850 °C for 4 h is less than 0.3%. Polypropylene–polyethylene (6%) copolymer (PP) was supplied by Atofina-France (polypropylene 9760).

## 2.2. Fillers treatment

To reduce the lignin content different treatments are carried out and different fractions are obtained. Four hundred grams of LF are added under stirring to 3 L of NaOH 2 N. This extraction is carried out at one of the three following conditions:

- C1 – aqueous medium at room temperature,
- C2 – aqueous medium at reflux,
- C3 – organic medium (ethanol 48%) at reflux.

These treatments combine a degradation of the 3D Lignin structure with a solubilisation and an extraction of the corresponding degraded products. The kinetics of the lignin solubilisation in the liquid media by UV has been followed. Fig. 4 shows that the absorption spectra of the solutions obtained after different extraction time present two main maxima, at 280 and 320 nm. Recording the solution absorbance at these two wavelengths allows to follow the lignin extraction kinetics, as shown in Fig. 5. After 2 h, the lignin concentration is stabilized. Then, to avoid a deep degradation of the lignocellulose materials, the total treatment time is fixed at 2 h for each of the three conditions (C1, C2 or C3).

After the lignin solubilisation, the insoluble fraction is filtered, recovered and washed several times with distilled water. The conductivity of the filtrate is determined after each washing. When the conductivity is close to the

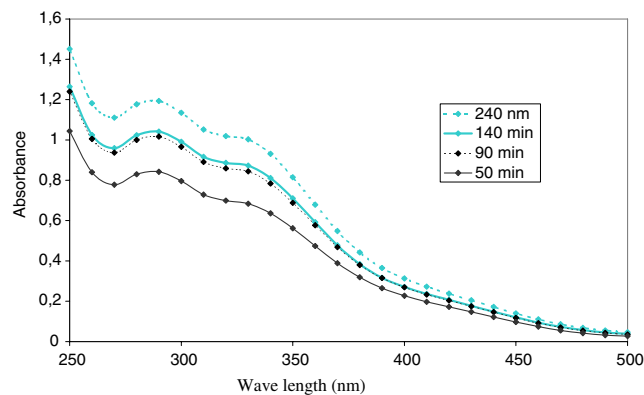


Fig. 4. UV absorption spectra recorded after different extraction time (from 240 to 50 min).

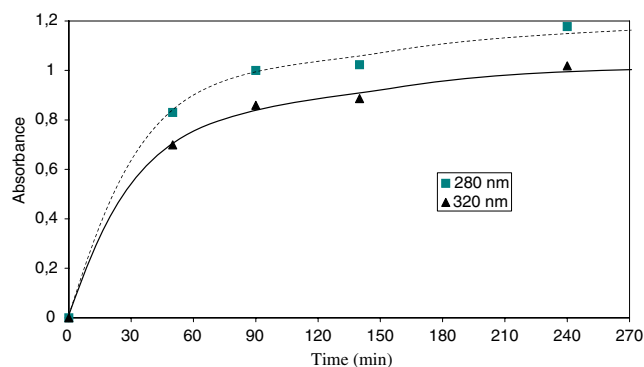


Fig. 5. Kinetics of lignin extraction determined by UV absorbance spectra at 280 and 320 nm.

distilled water value, the insoluble fraction is then washed with ethanol (40%). The wet fractions are dried in an air-circulating oven for one night at 80 °C. The dried powder is physically grinded to eliminate most of the aggregates. Afterwards the fillers are sieved to recover the residual agglomerates which are physically grinded. These operations are reiterated till all the aggregates are eliminated. According to the treatments (C1, C2 or C3), three different fillers fractions (TLF<sub>1</sub>, TLF<sub>2</sub> or TLF<sub>3</sub>) are obtained, respectively.

### 2.3. Biocomposites processing

In a previous publication (Le Digabel et al., 2004), we have shown that the interactions between the lignocellulose fillers and PBAT are sufficient enough to avoid addition of compatibilizers. Besides, we have shown that the fillers degradation temperature is much higher than the processing temperature. By determining Mw and IP by SEC, we have also shown that the matrix does not significantly degrade during the processing steps under thermo-mechanical treatments. Prior to blending, fillers and thermoplastic granules are dried in an air-circulating oven at 80 °C, for up to 4 and 1 h, respectively. PBAT and varying amounts of lignocellulose fillers are directly added into the feeding zone of a single screw extruder (SCAMIA S 2032, France) equipped with a specific designed torpedo-like element to promote high shearing and mixing. The screw diameter (D) and the L/D ratio are 30 mm and 26/1, respectively. For technical reasons due to the quality of the dispersion, a maximum fillers content of 30 wt% is added. Extrusion temperature is 135 °C. After air-cooling, 3-mm diameter strands are pelletized. These granules are extruded once again in the same conditions to improve the fillers dispersion into the matrix.

Standard dumbbell specimens (NFT 51-034-1981) are moulded with an injection moulding machine (DK codim NGH 50/100) in a temperature range between 115 and 130 °C, with an injection pressure and speed of 500 bars and 50 mm/s. Holding pressure and holding times are 500 bars and 12 s (PBAT) or 14 s (biocomposites), respectively. Mould temperature is 30 °C. The total cooling time

is 22 s (neat PBAT) and 24 s (biocomposites). The injection-moulded specimens are approximately 10 mm wide and 4 mm thick on the central part (French standard NFT 51-0.34 1981).

### 2.4. Characterisations

PBAT molecular weight and polydispersity index are determined by SEC with PS standards for the calibration. Analyses are performed in THF on two PL-gel 5 µm mixed-C, a 5 µm 100 Å and a 5 µm Guard columns in a Shimadzu LC-10AD liquid chromatograph (Japan) equipped with a Shimadzu RID-10A refractive index detector and a Shimadzu SPP-M10A diode array UV detector.

The size distribution of the fillers is determined by light scattering with a particles size analyzer in a 10 nm to 2 mm range (Mastersizer 2000, Malvern Instruments – UK).

The composition of the fillers is determined with several methods. Lignin content is measured by Klason method according to the protocol described by Monties (1984). For each sample 300 mg (M) are added to 3 ml H<sub>2</sub>SO<sub>4</sub> (72%). After 2 h at 20 °C, the solution is diluted into 40 ml of distilled water. Then, the mixing is carried out at reflux for 3 h. After filtration, the solid residue is washed several times with distilled water until neutrality of the filtrate. The residue is dried at 100 °C for 20 h and weighted (P<sub>1</sub>). This residue is calcinated at 500 °C for 210 min and then weighted (P<sub>2</sub>) to determine the mineral content. The measurements are triplicated for each tested sample. The lignin content is calculated according to Eq. (1).

$$\text{Lignins (KL)} = \frac{P_1 - P_2}{M} \quad (1)$$

After acid hydrolysis (H<sub>2</sub>SO<sub>4</sub>) and filtration to eliminate lignin and minerals, sugar titration allowed quantifying the cellulose and hemicellulose contents according to the procedure described by Lequart, Ruel, Lapierre, Pollet, and Kurek (2000). This analysis is carried out with high performance liquid chromatography (HPLC) with a Dionex<sup>®</sup> column (anion exchange column). During the analysis, the different dissolved sugars are ionized with NaOH (0.1 N) which is the mobile phase. The glucose concentration gives the cellulose content. The different sugars obtained from hemicellulose hydrolysis are also quantified.

Contact angle measurements are carried out with a goniometer (Kruss G23, Germany). Surface tensions of solid materials are calculated from the sessile drop method. Water (W), formamide (F) and methylene iodide (MI) are used as test liquids because of their different polarities. From the contact angles values, different models can be developed to determine the surface parameters (Le Digabel, 2004). In the present case, Wu's method (Wu, 1982) is used to evaluate the polar (γ<sup>p</sup>) and dispersive (γ<sup>d</sup>) components of the surface tension (γ) according to Eq. (2).

$$\gamma = \gamma^p + \gamma^d \quad (2)$$

The harmonic-mean equation Eq. (3) is used to calculate the work of adhesion ( $W_{12}$ ) between the matrix (1) and the natural fibers (2). The interfacial tension ( $\gamma_{12}$ ) is then calculated (Wu, 1982) according to Eq. (4).

$$W_{12} = \frac{4\gamma_1^d\gamma_2^d}{\gamma_1^d + \gamma_2^d} + \frac{4\gamma_1^p\gamma_2^p}{\gamma_1^p + \gamma_2^p}, \quad (3)$$

$$\gamma_{12} = \gamma_1 + \gamma_2 - W_{12}. \quad (4)$$

Measurements are carried out on tablets (200 mg) moulded under vacuum at room temperature for the fillers. The tests are performed on injected dumbbell specimens for the matrices.

Differential scanning calorimeter (DSC 2920 and 2910, TA Instruments, USA) is used for thermal characterizations. Samples (between 10 and 15 mg) are sealed in aluminium pans. The heating and cooling rates are  $10\text{ }^\circ\text{C min}^{-1}$ . A nitrogen flow ( $45\text{ ml min}^{-1}$ ) is maintained during the test. For all materials, the first scan is used for discarding the thermal history of the material. Each sample is heated to  $150\text{ }^\circ\text{C}$  then cooled to  $-50\text{ }^\circ\text{C}$  before a second heating scan to  $150\text{ }^\circ\text{C}$ . The glass transition temperature ( $T_g$ ) and melting temperature ( $T_m$ ) are determined from the second heating scan. The crystallisation temperature ( $T_c$ ) is obtained from the cooling scan because the samples were not quenched. The temperature of induction ( $T_i$ ) is the beginning of the crystallisation during the cooling.  $T_g$  is determined at the mid-point of heat capacity changes,  $T_m$  at the onset of the endothermic peak and  $T_c$  at the onset of the exothermic peak. Three samples of each blend are analysed. By integration of the corresponding peaks we have determined the different heats of crystallization and fusion ( $\Delta H_c$  and  $\Delta H_f$ ). These values determined in J/g can be corrected from a diluent effect linked to the fillers incorporation into the matrix according to the Eqs. (5) and (6) where  $w$  is the fillers fraction.

$$\Delta H'_c = \frac{\Delta H_c}{1 - ww}, \quad (5)$$

$$\Delta H'_f = \frac{\Delta H_f}{1 - ww}. \quad (6)$$

The degree of crystallinity (in %) can be estimated with Eq. (7).  $\Delta H_{100\%}$  has been estimated at  $114\text{ J/g}$ , for PBAT according to the method presented by Herrera, Franco, Rodriguez-Galan, and Puiggali (2002).

$$X_c(\%) = \frac{\Delta H'_f}{\Delta H_{100\%}}. \quad (7)$$

Tensile testing is carried out with an Instron tensile testing machine (model 4204) with a crosshead speed of  $50\text{ mm/min}$ , according to the ASTM D882-91. Ten samples for each formulation are tested. Before testing, the different specimens are stabilized. The storage conditions are  $23\text{ }^\circ\text{C}$  and  $50\%$  RH (relative humidity) for 5 days. The non-linear mechanical behaviour of the samples is determined through different parameters. The nominal and the true strains are given by Eqs. (8) and (9), respectively. In these equations,

$L$  and  $L_0$  are the length during the test and at zero time, respectively. Two different strains are calculated; strain at the yield point ( $\varepsilon_Y$ ) and at break ( $\varepsilon_b$ ).

$$\langle \varepsilon \rangle = \frac{L - L_0}{L_0}, \quad (8)$$

$$\varepsilon = \text{Ln}\left(\frac{L}{L_0}\right). \quad (9)$$

The nominal stress is determined by Eq. (10) where  $F$  is the applied load and  $S_0$  is the initial cross-sectional area. The true stress is given by Eq. (11) where  $F$  is the applied load and  $S$  is the cross-sectional area.  $S$  is estimated assuming that the total volume of the sample remained constant, according to Eq. (12). Both, stress at the yield point ( $\sigma_Y$ ) and at break ( $\sigma_b$ ) are determined.

$$\langle \sigma \rangle = \frac{F}{S_0}, \quad (10)$$

$$\sigma = \frac{F}{S}, \quad (11)$$

$$S = S_0 \times \frac{L_0}{L}. \quad (12)$$

Young's modulus ( $E$ ) is measured from the slope of the low strain region (Nielsen & Landel, 1994) in the vicinity of 0 ( $\sigma = \varepsilon = 0$ ).

### 3. Results and discussions

#### 3.1. Composition and granulometry of the treated fillers

Table 2 shows the different lignin contents determined by Klason titrations. After treatment the lignin content has decreased. Between TLF<sub>1</sub> and TLF<sub>3</sub> values, we can notice the effect of the temperature on the extraction. Extracted lignin content increases with the temperature. Between TLF<sub>2</sub> and TLF<sub>3</sub> values, the effect of the medium (aqueous vs. organic) is noticeable. Aqueous medium is much more efficient for extraction. This is partly due to the reflux temperature which is lower for the organic medium. Temperature seems to drive the extraction treatment. Depending on the treatment, a large range of lignin contents – from 30% (LF) to 14% (TLF<sub>2</sub>) – can be obtained.

Fig. 6 presents the size distributions of the different fractions (LF, TLF<sub>1</sub>, TLF<sub>2</sub> and TLF<sub>3</sub>) illustrating the influence of the treatment on the fillers granulometry. LF average size is  $315\text{ }\mu\text{m}$  but it seems to present a double distribution with a small population centred on  $50\text{ }\mu\text{m}$  and another one (greater) on  $630\text{ }\mu\text{m}$ . In a previous work (Le Digabel,

Table 2  
Granulometric data and lignins contents for the different fillers fractions

	LF	TLF <sub>1</sub>	TLF <sub>2</sub>	TLF <sub>3</sub>
Lignin content (%)	30	24	14	20
Distribution maxima ( $\mu\text{m}$ )	630	550	480	420
Average size ( $\mu\text{m}$ ) volume weighted	310	360	300	280

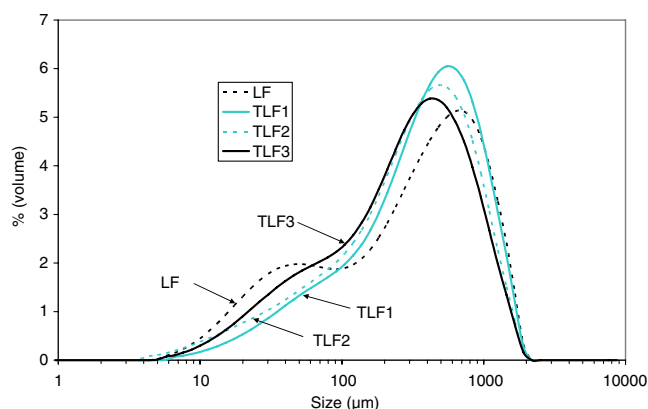


Fig. 6. Granulometric distributions of the different fillers fractions (LF, TLF<sub>1</sub>, TLF<sub>2</sub> and TLF<sub>3</sub>).

2004), we have shown that the first population (smallest size) presents higher lignin content. For this population, the total surface of the fillers is higher and then a greater quantity of lignin is available on the surface because the lignin is more easily accessible to be extracted on surface, during the fillers treatment. Fig. 6 shows that this fillers population centred on 50 µm is largely erased after treatment. The shape modification of the size distribution depends on the treatment of the fillers. Nevertheless, the size distributions obtained after the different treatments are more or less equivalent. Dissymmetric curves and thus duals populations are obtained. Table 2 shows the variations of the maxima on the size distributions from one fraction to another. We can notice a light decrease of the average sizes from TLF<sub>1</sub> to TLF<sub>3</sub>. To conclude, the different treatments seem partly to modify both the fillers average size and the population distribution.

### 3.2. Surface and interfacial properties

The surface properties of the different fillers are analysed by surface tension determinations. We can measure the contact angles by liquid drop depositions on the materials surface. Table 3 gives the contact angle measurement determined with water (W), formamide (F) and methylene iodide (MI). We can notice that the standard deviations

of the results are rather important for measurements. This is due to the light roughness of the surface for some samples.

On the one hand, PP – the hydrophobic reference material – logically presents the highest contact angle with water. On the other hand, cellulose gives the lowest contact angle linked to its high hydrophilic nature. According to the lignin contents, we could assume that TLF shows values between LF and CF data but in fact it is not the case. The different treatments induce an increase of the contact angles, more particularly for TLF<sub>3</sub>. In this last case, we show a kind of hydrophobisation of the surface which is highlighted by a water contact angle close to 90°, close to PP value. Some rearrangements between the parietal compounds or chemical reactions can take place leading to a hydrophobic surface. For example, some ionized phenolic compounds (from lignin) can react with cellulose or residual hemicellulose, under the treatment conditions of these fillers.

From these contact angles, we can obtain the surface energy. Table 3 shows the values of the different surface component which are determined from the contact angles according to Wu's method (Wu, 1982), with different liquids couples (W/MI and MI/F). We can notice that the results obtained with both liquids couples are close. Dispersive components vary only from 28 to 40 mJ/m<sup>2</sup> whereas polar components vary in a large scale from 2 to 22 mJ/m<sup>2</sup>. These variations are related to the polar or non-polar character of the substrates. The hydrophobic character of TLF<sub>3</sub> is pointed out by its low polar component, like PP. But, the other fillers show relatively high values in agreement with their hydrophilic character. TLF<sub>1</sub> shows values close to LF. We can consider that TLF<sub>2</sub> exhibits dispersive and polar components comparable to CF. These last results could be due to a low residual lignin concentration on the fillers surface.

Table 4 gives the calculated work of adhesion and interfacial tension for various hypothetical biocomposites based on PBAT. The work of adhesion values are comprised between 82 and 109 mJ/m<sup>2</sup>. Except for TLF<sub>3</sub> which exhibit a hydrophobisation of the surface, we can observe an increase in the interfacial tension from LF to CF according

Table 3  
Surface tensions data of the different components (fillers and matrices) obtained from contact angle measurements

	W (°)	MI (°)	F (°)	Dispersive component ( $\gamma^d$ in mJ/m <sup>2</sup> )		Polar component ( $\gamma^p$ in mJ/m <sup>2</sup> )		Surface tension ( $\gamma$ in mJ/m <sup>2</sup> )	
				W/MI	MI/F	W/MI	MI/F	W/MI	MI/F
LF	62 (8)	45 (1)	51 (4)	33	33	16	12	49	45
TLF <sub>1</sub>	62 (3)	55 (2)	61 (1)	28	29	18	10	46	39
TLF <sub>2</sub>	69 (5)	52 (2)	70 (6)	40	40	25	20	65	60
TLF <sub>3</sub>	84 (4)	54 (3)	73 (1)	30	30	7	5	37	35
CF (cellulose)	47 (2)	31 (2)	16 (2)	38	38	22	20	60	58
PBAT	65 (2)	30 (2)	45 (2)	39	40	13	11	52	51
PP (hydrophobic ref.)	96 (2)	53 (2)	78 (2)	31	32	3	2	34	34

Note: Standard deviations are given in parenthesis.

Table 4  
Works of adhesion and interfacial tensions for PBAT-based biocomposites

	PBAT/LF	PBAT/TLF <sub>1</sub>	PBAT/TLF <sub>2</sub>	PBAT/CF	PBAT/TLF <sub>3</sub>
Lignin content (%)	30	24	14	0	20
Work of adhesion (mJ/m <sup>2</sup> )	95	88	109	106	82
Interfacial tension (mJ/m <sup>2</sup> )	0.71	1.80	2.63	2.66	3.68

Note: These values are determined with the liquids couple “MI/F”.

to the decrease of the lignin content. Tables 3 and 4 show the same type of results i.e., TLF<sub>2</sub> and CF-based materials present comparable values.

### 3.3. Thermal properties

Table 5 gives main DSC thermal characteristics. Compared to most thermoplastics,  $T_g$  and  $T_f$  of PBAT are rather low and therefore the processing temperature is low too, around 130 °C. PBAT is at room temperature between  $T_g$  and  $T_f$  i.e., on the rubber plateau. PBAT crystallinity is quite low, around 12%. We can notice that the  $\Delta C_p$  at the glass transition is low, too. The different thermodynamic values are consistent with values obtained by other authors (Herrera et al., 2002).

Table 5 presents the different data obtained by DSC on PBAT-based materials with different kind of fillers at the same content (30 wt%). Concerning the fillers and the corresponding bio-composites, the results with the fillers which exhibit the highest (LF) and lowest (TLF<sub>2</sub>) lignin contents are only shown. The addition of the fillers (treated or untreated) induces a slight but significant increase in  $T_g$ , from  $-39.3$  to  $-35.7$  °C. According to Avella et al. (2000), this trend may be explained by intermolecular interactions between the fillers hydroxyl groups and the carbonyl groups of the PBAT ester functions. These hydrogen bonds would probably reduce the polymer mobility and then increase  $T_g$  values. PBAT/TLF<sub>2</sub> shows intermediate  $T_g$  value between neat PBAT and PBAT/LF data as a possible consequence of the treatment on the fillers surface. Then, the fillers–matrix interactions seem to be more important for untreated fillers. These results could be correlated to the surface energy data (Table 4) since PBAT/LF shows the lowest interfacial tension.

Compared to the matrix, the biocomposites do not show important variation of  $T_f$ . This is in agreement with SEC determinations since we have not detected any significant chains length variations linked to chains degradation phenomena that could occur under the thermo-mechanical treatments during the composite processing.

Table 5  
DSC results of PBAT and PBAT-based biocomposites

Samples	$T_g$ (°C)	$T_c$ (°C)	$\Delta H_c$ (J/g)	$\Delta H'_c$ (J/g)	$T_f$ (°C)	$\Delta H_f$ (J/g)	$\Delta H'_f$ (J/g)	$X_c$ (%)
PBAT	$-39.3$ (0.3)	68.0 (1)	13.5 (0.2)	13.5 (0.2)	113.9 (0.5)	13.9 (0.3)	13.9 (0.3)	12
PBAT-30% LF	$-35.7$ (0.2)	70.7 (0.3)	9.3 (0.5)	13.3 (0.7)	112.2 (0.6)	10.0 (0.3)	14.2 (0.4)	12
PBAT-30% TLF <sub>2</sub>	$-36.4$ (0.2)	73.0 (0.1)	9.2 (0.2)	13.1 (0.2)	114.2 (0.1)	10.6 (0.1)	15.1 (0.1)	13

Note: Standard deviations are given in parenthesis.

The corrected values of heats of crystallization and fusion are quite equivalent. The heats of crystallization and fusion are between 13 and 15 J/g. We only have very small crystallisation during the second heating scan. The incorporation of the fillers induces a slight but significant increase in  $T_c$  that is probably linked to the reduction of the polymer mobility and to a nucleation effect linked to the fillers surface. The increase of  $T_c$  is much more important for TLF<sub>2</sub> compared to LF. This may be due to the roughness of the fillers surface which is increased by the NaOH treatment and which enhances a nucleation effect although the fillers–matrix interactions (hydrogen bonds) are lower for treated fillers. We can notice that the addition of treated or untreated fillers to the matrix does not significantly affect the PBAT degree of crystallinity which stays constant at around 12–13%.

### 3.4. Mechanical properties

The matrix (PBAT) mechanical parameters are given in Table 6. These values are in agreement with  $T_g$  and  $T_f$  values. PBAT is a ductile material at room temperature. All the mechanical results (Figs. 7–9) are based on the addition of 30 wt% fillers fractions into the PBAT matrix. Fig. 7 gives the different Young's modulus results. The stiffness of the biocomposites is 4–5.5 times the value of the neat PBAT modulus. Compared to PBAT/LF biocomposites, the incorporation of treated fillers involves an increase of the modulus. Although we cannot notice any linear relations between the modulus and the lignin content, the modulus evolution from LF to TLF<sub>2</sub> is linked to the enrichment in cellulose. This effect is more particularly shown with TLF<sub>2</sub>-based composites which present a very low lignin

Table 6  
PBAT tensile test results

Modulus (MPa)	Yield stress (MPa)	Strength at break (MPa)	Elongation at the yield point (%)	Elongation at break (%)
$E$	$\sigma_Y$	$\sigma_b$	$\varepsilon_Y$	$\varepsilon_b$
40	8	>84	28	>200

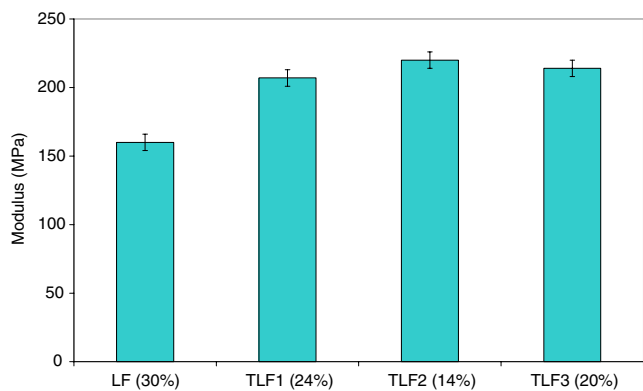


Fig. 7. Young's modulus of PBAT-based biocomposites with different fillers fractions (LF, TLF<sub>1</sub>, TLF<sub>2</sub> and TLF<sub>3</sub>).

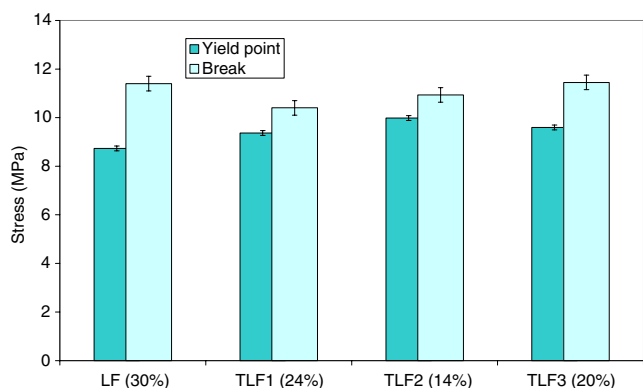


Fig. 8. Stresses at Yield point and break of PBAT-based biocomposites with different fillers fractions (LF, TLF<sub>1</sub>, TLF<sub>2</sub> and TLF<sub>3</sub>).

content on the surface according to the surface tension results.

Figs. 8 and 9 present the results of stress and elongation, both at yield point and at break. At the yield point, the treated fillers present both higher stresses and lower strains, compared to LF fillers. These values are in agreement with the rigidification of the fillers linked to higher cellulose contents. Nevertheless, we cannot notice any significant variation of the results between differently treated fillers (TLF<sub>1-3</sub>).

Stresses at break for the different biocomposites are more or less equivalent. TLF<sub>1</sub> and TLF<sub>2</sub>-based biocomposites show the smallest values. Compared to LF composites, we observe a decrease of the strain at break with the treated fillers. TLF<sub>1</sub> and TLF<sub>2</sub>-based composites show equivalent results. TLF<sub>3</sub> shows intermediate values between LF and TLF<sub>1</sub> or TLF<sub>2</sub>-based biocomposites. This result is not in agreement with data obtained from contact angle measurements. These results can be partially explained by the modification of the fillers granulometric distribution in the range of the lowest sizes (Fig. 6). In a previous work (Le Digabel, 2004), we have seen that the smallest population mainly drives the mechanical results at break. The smallest fillers sizes tend to increase the elongation and the stress at break, compared to the biggest ones. In the range of the smallest

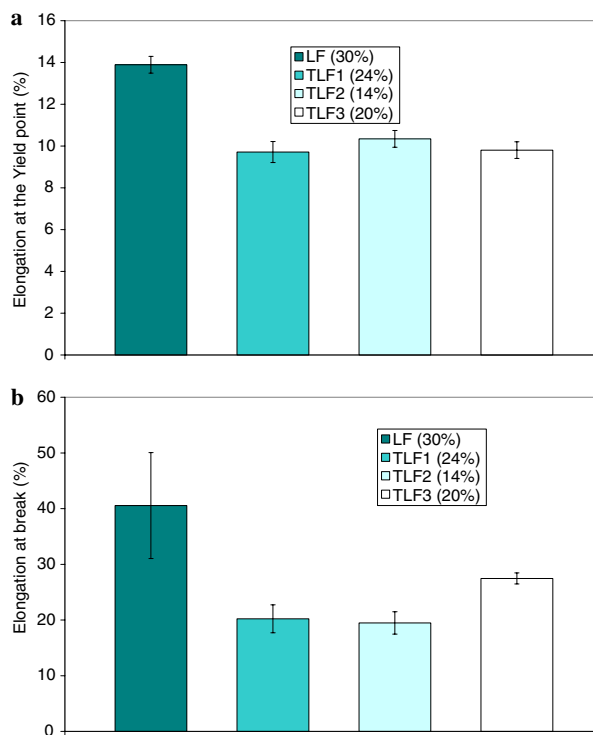


Fig. 9. Elongation at yield point (a) and break (b) of PBAT-based biocomposites with different fillers fractions (LF, TLF<sub>1</sub>, TLF<sub>2</sub> and TLF<sub>3</sub>).

sizes, TLF<sub>3</sub> presents intermediate distribution between TLF<sub>1</sub> or TLF<sub>2</sub> and LF. In conclusion, we can notice that these mechanical results are not in full agreement with the data obtained from contact angle measurements. It is mainly because the tension surface does not completely take into account some factors or phenomena as e.g., the fillers shape (granule vs. rods for the biggest particles) or the fillers fibrillation (Le Digabel, 2004) which play a great role in mechanical properties.

#### 4. Conclusion

Different biocomposites (biodegradable composites) have been produced by incorporation of lignocellulose fillers into a biodegradable aromatic polyester, polybutylene adipate-co-terephthalate. The paper is focused on the analysis of the behaviour of biocomposites reinforced with fillers fractions which present lignin content variation. These materials have been carried-out by extrusion and injection moulding. The lignocellulose fillers are a by-product of an industrial fractionation process based on wheat straw. From the raw agro-material, various fillers fractions (TLF<sub>1</sub> to TLF<sub>3</sub>) have been obtained by selecting different fractionation conditions to extract the lignin according to the liquid media (water or ethanol) and the temperature (room temperature and at solvent reflux). The consequent lignin content varies from 30 to 14 wt% with an inverse evolution of the cellulose content. These treatments have partially modified the granulometry distribution with a decrease of the smallest fillers population. Major effect is observed on the fillers surface tensions. We



have achieved a large range of behaviour since we have obtained rather hydrophobic fillers (TLF<sub>3</sub>) or highly hydrophilic fillers (TLF<sub>2</sub>). Nevertheless, TLF<sub>1</sub> surface properties are close to the initial fillers (LF). The effect of the fillers fractions variations on the thermal properties is particularly notable on the PBAT crystallization temperature. This effect could be linked to the increase in the fillers roughness after treatment which could be partially due to a fibrillation phenomenon. Nevertheless, no significant influence of the different fillers has been observed on the PBAT crystallinity. Concerning the mechanical properties, we can note an effect of the different fillers treatments linked not only to the evolution of the fillers composition but also, to the granulometric distributions and to the fillers surface. The increase of the biocomposites moduli are mainly linked to the fillers cellulose content. Although stresses at break are more or less equivalent for the different biocomposites, we can observe an increase of the stress at the yield point according to the treatment of the fillers. The elongations at break and at the yield point decrease from LF to treated fillers (TLF)-based biocomposites. In the explored domain i.e., according to the tested fillers, we have obtained a large range of mechanical properties. These different behaviours can fulfil the requirements for different applications, such as non-food packaging or other short-lived applications (agriculture, sport ...) where long-lasting polymers are not entirely adequate.

In further investigations, we plan to analyse the impact of the lignin content on the material biodegradability. Besides, taking into account the well known variability of lignin (Monties, 1998) and the natural biological variability of agricultural products, we should expect large variations of the chemomechanical properties of the corresponding biocomposites.

### Acknowledgements

This work was funded by Europol'Agro through a research program devoted to materials based on agricultural resources. The authors want to thank Pr. Monties for his great investment in this project.

### References

- Avella, M., La Rota, G., Martuscelli, E., Raimo, M., Sadocco, P., Elegir, G., et al. (2000). Poly(3-hydroxybutyrate-co-3-hydroxyvalerate) and wheat straw fibre composites: thermal, mechanical properties and biodegradation behaviour. *Journal of Materials Science*, 35(4), 829–836.
- Avérous, L. (2004). Biodegradable multiphase systems based on plasticized starch: a review. *Journal of Macromolecular Science—Part C, Polymer Reviews*, C4(3), 231–274.
- Avérous, L., & Boquillon, N. (2004). Biocomposites based on plasticized starch: thermal and mechanical behaviours. *Carbohydrate Polymers*, 56(2), 111–122.
- Avérous, L., Fringant, C., & Moro, L. (2001). Plasticized starch–cellulose interactions in polysaccharide composites. *Polymer*, 42(15), 6571–6578.
- Bledzki, A. K., & Gassan, J. (1999). Composites reinforced with cellulose-based fibres. *Progress in Polymer Science*, 24, 221–274.
- Herrera, R., Franco, L., Rodríguez-Galan, A., & Puiggali, J. (2002). Characterization and degradation behavior of poly(butylene adipate-co-terephthalate)s. *Journal of Polymer Science: Part A: Polymer Chemistry*, 40, 4141–4157.
- Kitagawa, K., Watanabe, D., Mizoguchi, M., Hamada, H. (2002). Bamboo particle filled composites. *Polymer Processing Symposium PPS-18*, Guimares (Portugal).
- Le Digabel, F., Boquillon, N., Dole, P., Monties, B., & Avérous, L. (2004). Properties of thermoplastic composites based on wheat straw lignocellulosic fillers. *Journal of Applied Polymer Science*, Vol. 93(N°1), 428–436.
- Le Digabel, F. (2004). *Incorporation de co-produits de paille de blé dans des matrices thermoplastiques. Approche de la compatibilité charge-matrice et propriétés des composites*. Ph.D. Thesis URCA Reims (France). p. 196.
- Lequart, C., Ruel, K., Lapierre, C., Pollet, B., & Kurek, B. (2000). Abiotic and enzymatic degradation of wheat straw cell wall: a biochemical and ultrastructural investigation. *Journal of Biotechnology*, 80, 249–259.
- Mohanty, A. K., Misra, M., & Hinrichsen, G. (2000). Biofibres, biodegradable polymer and composites: an overview. *Macromolecular Material Engineering*, 276/277, 1–24.
- Monties, B. (1984). Dosage de la lignine insoluble en milieu acide. *Agronomie*, 4, 387–392.
- Monties, B. (1998). Novel structures and properties of lignin in relation to their natural and induced variability in ecotypes, mutants and transgenic plants. *Polymer Degradation and Stability*, 59, 53–64.
- Netravali, A. N., & Chabba, S. (2003). Composites get greener. *Materials Today*, 6(4), 22–29.
- Nielsen, L. E., & Landel, R. F. (1994). *Mechanical properties of polymers and composites*. New York: Marcel Dekker.
- Rouilly, A., & Rigal, L. (2002). Agro-materials: a bibliographic review. *Journal of Macromolecular Science—Part C, Polymer Reviews*, C42(4), 441–479.
- Roller, M. (1990). *Valorisation non alimentaire des co-produits du blé: contribution à l'extraction et à la purification d'hexoses et de pentoses en vue de la synthèse de polyglycosides d'alkyles*. PhD Thesis Paris Grignon (France). p. 214.
- Saheb, D. N., & Jog, J. P. (1999). Natural fiber polymer composites: a review. *Advances in Polymer Technology*, 18(4), 351–363.
- Sun, R., Lawther, J. M., & Banks, W. B. (1997). A tentative chemical structure of wheat straw lignin. *Industrial Crops and Products*, 6, 1–8.
- Wollendorfer, M., & Bader, H. (1998). Influence of natural fibres on the mechanical properties of biodegradable polymers. *Industrial Crops and Products*, 8, 105–112.
- Wu, S. (1982). *Polymer interface and adhesion*. New York: Marcel Dekker.
- Young, R. A. (2004). *Vegetable fibers*. *Encyclopedia of polymer science and technology*, In Herman F. Mark (Ed.) Vol. 12. John Wiley & Sons, Inc.